Supplementary information

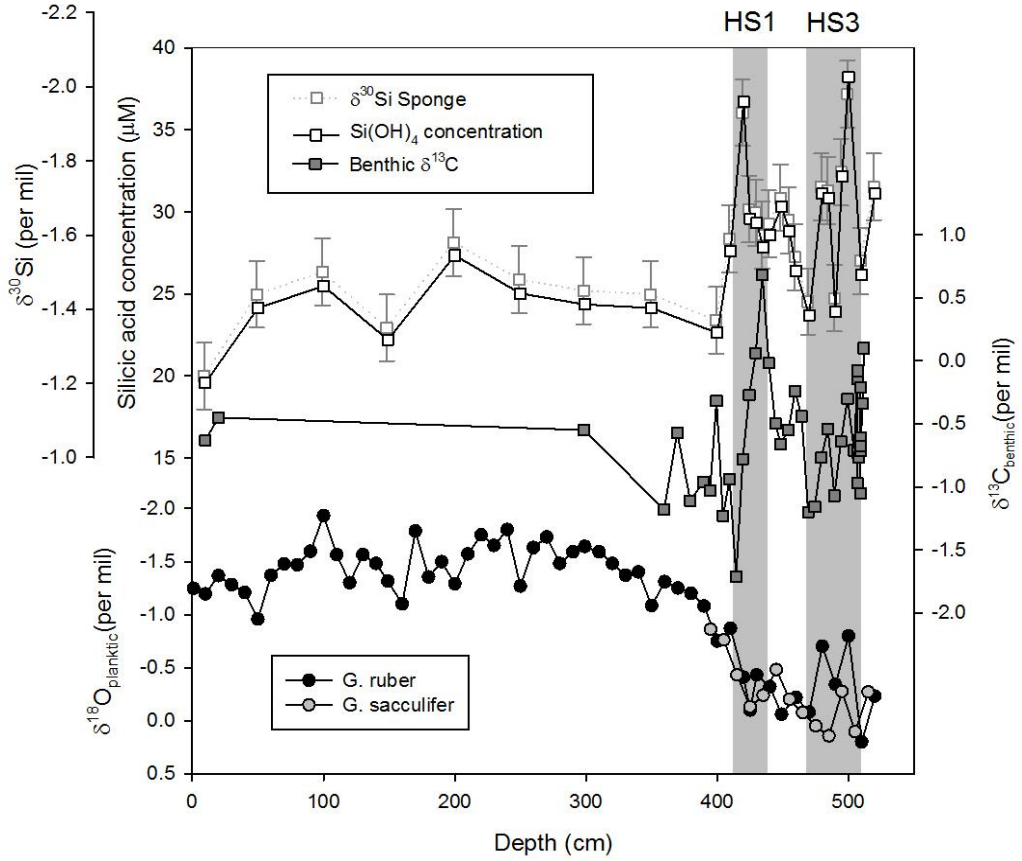

Supplementary Figure 1: Benthic nutrient proxies for sediment core KNR140-2-56GGC. The hollow squares show the sponge spicule δ^{30}Si composition (error bars show $\pm 2\sigma_{SD}$) and the reconstructed $Si(OH)_4$ concentration, calculated assuming $[Si(OH)_4]=270/(\Delta\delta^{30}Si+6.54)-53$ [23], where $\Delta\delta^{30}$Si is the difference in isotopic composition of the sponge spicules and seawater and assuming $\delta^{30}Si(OH)_4$ of dissolved silicon in seawater is +1.6‰ [53]. The solid grey squares show uncorrected δ^{13}C records from the benthic foraminifera *Uvigerina peregrina*. The circles show planktonic foraminifera δ^{18}O records [27]. The δ^{30}Si values of Holocene (samples younger than 10 ka BP, 0-400 cm) spicules extracted from KNR140-2-56GGC were significantly heavier than samples deeper than 400 cm (Wilcoxon-Mann-Whitney-U test for n_1=9 and n_2=17, one-tail test P<0.0005, two-tailed test P<0.001). Note that the light spicule δ^{30}Si peaks at HS1 and HS3 approximately correspond to light benthic foraminifera δ^{13}C values, consistent with switches between partially southern sourced (lighter δ^{13}C; higher $Si(OH)_4$) to predominantly northern sourced (heavier δ^{13}C ; lower $Si(OH)_4$). The corresponding peaks vary slightly in depth down the core, which could reflect the different mixing properties in sediments of spicules and benthic foraminifera. Figure 2 (main text) and Supplementary Fig. 1 also highlights the change in sedimentation rate at the deglaciation, which could be a result of change in water mass and/or change in flow speed. However, a depth transect of benthic proxy data would be required to determine whether the observations were a result of a vertical or lateral shift in northern versus southern component waters.

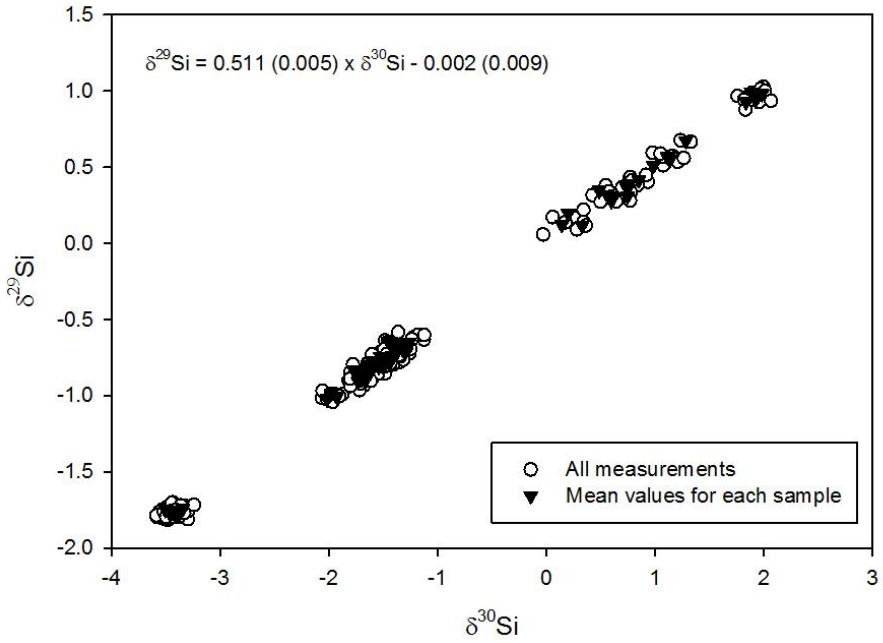

Supplementary Figure 2: Three-isotope plot of all silicon isotope data used in this study. The hollow symbols show all individual measurements; the solid symbols show the mean values (typically n=3) for each sample. The gradient of the slope is consistent with equilibrium fractionation.

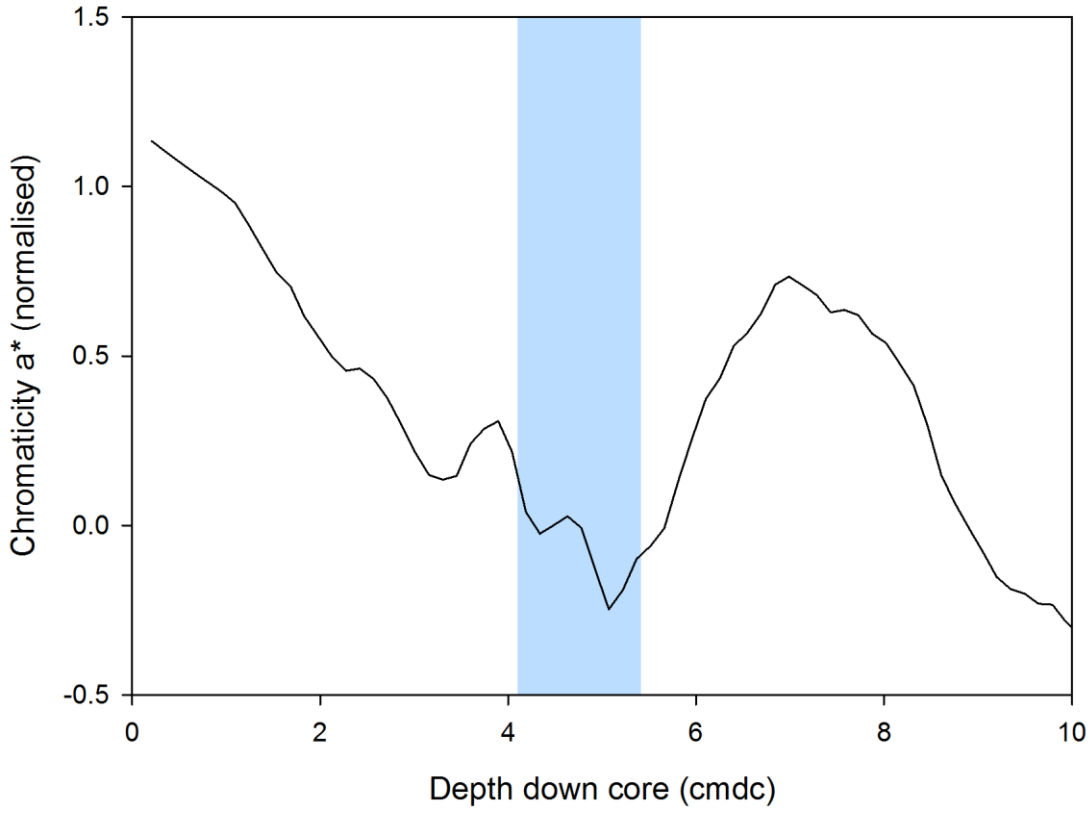

Supplementary Figure 3: Reflectance data for core ODP172-1054B. Core ODP172-1054B is ~100m shallower than KNR140-2-56GGC on the Carolina Slope (adapted from [27]). The data have been smoothed using Sigmaplot 12.5. The blue bar shows the depth range for KNR140-2-56GGC for the glacial section (pre-18 ka BP). Note the low red chromaticity, indicative of sediments from the Labrador Sea indicates that the Deep Western Boundary Current (DWBC) source of NADW/GNAIW was not influencing the site during the late glacial. However, it is possible that a northern sourced water mass that originated elsewhere in the northern high latitudes was present.

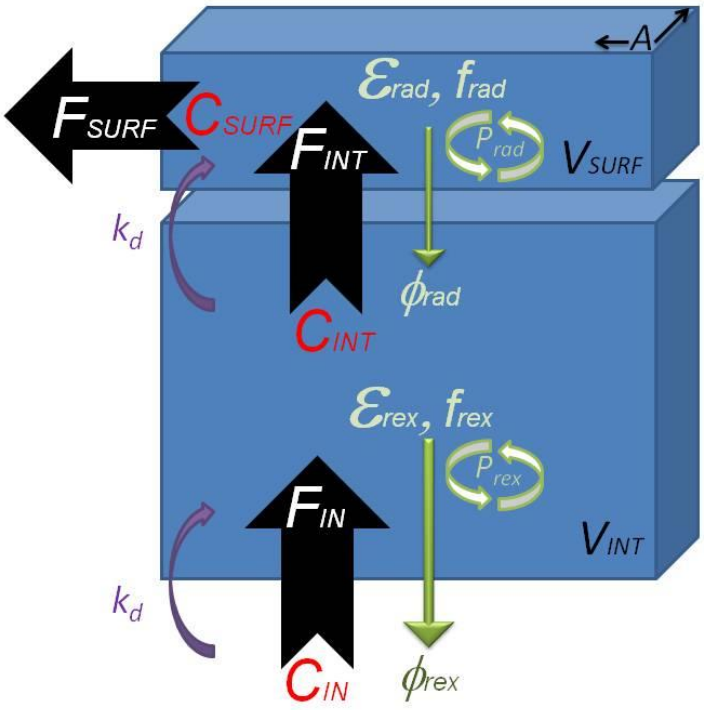

Supplementary Figure 4: Cartoon of the HS1 biogeochemical box model. Equations relating the parameters are reported in the methods section and symbols are defined in Supplementary Table 3.

A

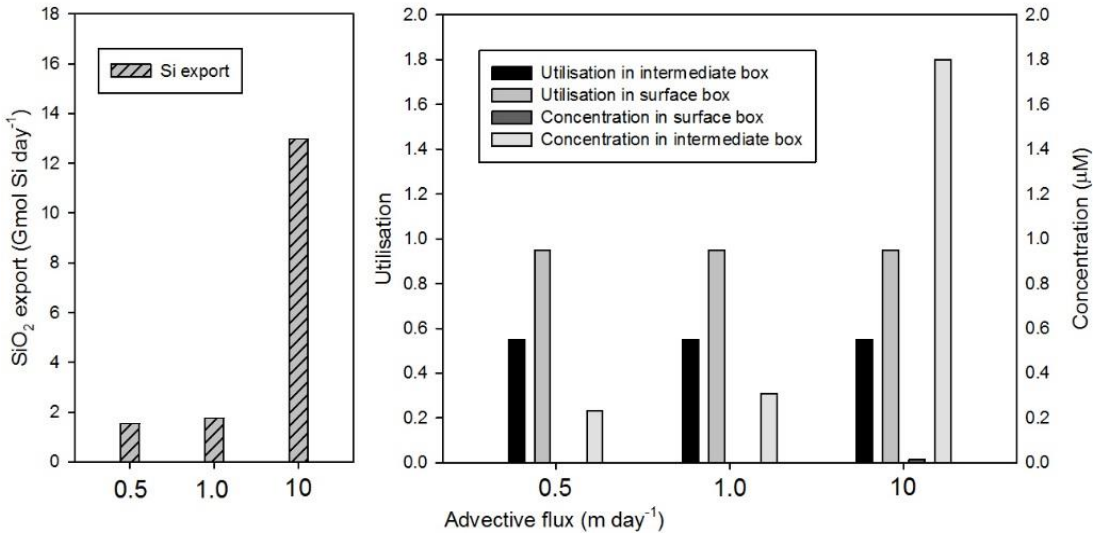

B

C

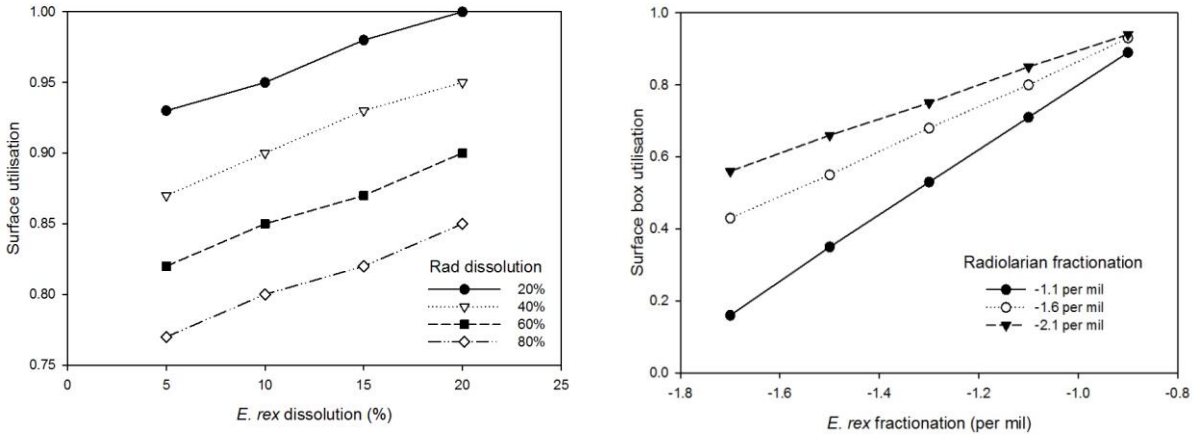

Supplementary Figure 5: Results of model tests. A shows the relationship between advective flux and opal export, utilization and $Si(OH)_4$ concentration; B shows the relationship between *E. rex* dissolution and surface utilization; and C shows the relationship between *E. rex* and radiolarian fractionation factor and surface utilization.

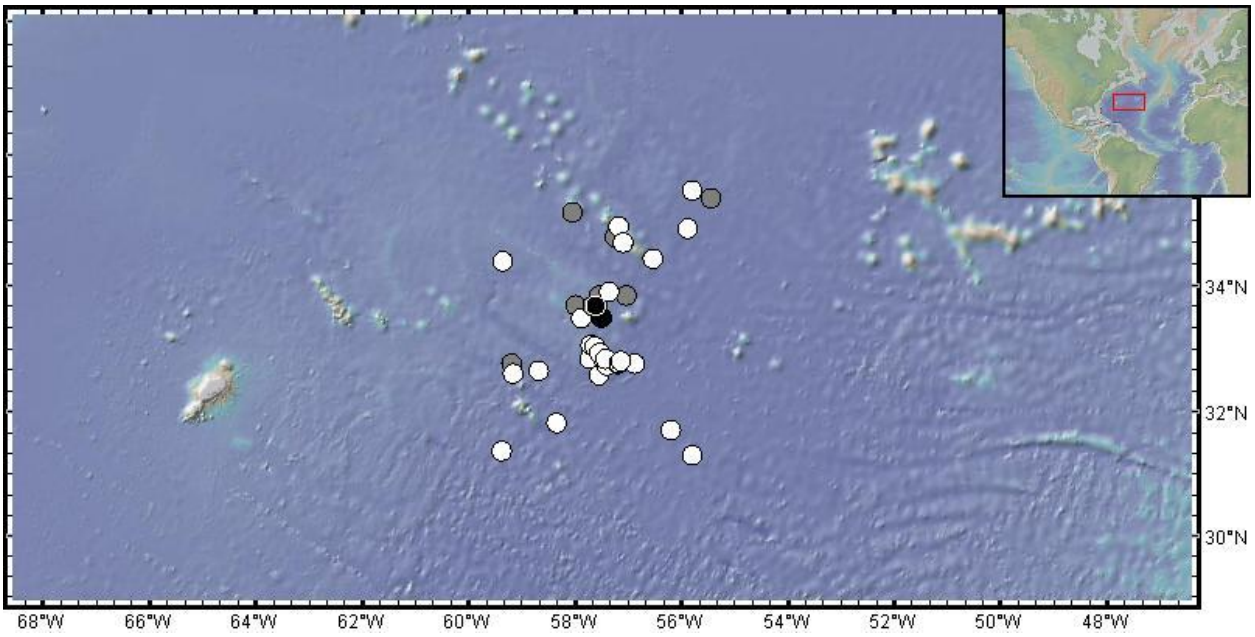

Supplementary Figure 6: A review of core descriptions from the North Atlantic in the National Geophysical Data Center [64] indicates that the occurrence of *E.rex* is limited to a small region around the Bermuda Rise. The solid circles show the location of *E.rex* layers during the deglacial; the grey circles show cores where there are noted increases in diatoms during the deglacial (>5%), and the white circles are cores where there are no increases in diatoms noted. Plot drawn using GeoMapApp.

Supplementary Table 1: Silicon isotope results for this study. *a* = sponge opal standard LMG08 (see [47]); *b* = measurements from HU-89038 that were not corrected by Mg-doping; *c* = ± numbers in parentheses give the range of values obtained from repeat measurements of each solution (n=2 or 3).

Sample	δ^{30}Si (‰)
LMG08[a]	
All Measurements (n=35)	-3.43 (2SD = 0.17)
Mean for each run (n=10)	-3.43 (2SD = 0.10)
HU-89038	
Bulk[b]	
360-370cm	0.86 (± 0.07[c])
460-470cm	0.41 (± 0.15)
E. rex	
330-340cm	0.85 (± 0.09)
340-350cm	0.75 (± 0.09)
360-370cm	0.99 (± 0.07)
370-380cm	0.56 (± 0.03)
380-390cm	0.76 (± 0.01)
390-400cm	1.14 (± 0.05)
430-440cm	0.14 (± 0.06)
440-450cm	0.75 (± 0.04)
450-460cm	0.49 (± 0.06)
460-470cm	0.33 (± 0.04)
470-480cm	0.20 (± 0.14)
480-490cm	0.60 (± 0.08)
Radiolarians	
330-340cm	1.98 (± 0.03)
340-350cm	1.93 (± 0.11)
360-370cm	1.88 (± 0.12)
370-380cm	2.00[b] (± 0.07)
380-390cm	1.63[b] (± 0.17)
430-440cm	0.73 (± 0.04)
440-450cm	1.11 (± 0.12)
460-470cm	1.13 (± 0.11)
470-480cm	1.28 (± 0.05)
480-490cm	1.84 (± 0.02)

KNR140-2-GC56

10cm	-1.22 (± 0.10)
50cm	-1.44 (± 0.17)
100cm	-1.50 (± 0.06)
150cm	-1.35 (± 0.10)
200cm	-1.58 (± 0.07)
250cm	-1.48 (± 0.06)
300cm	-1.45 (± 0.04)
350cm	-1.44 (± 0.05)
400cm	-1.37 (± 0.05)
410cm	-1.59 (± 0.05)
420cm	-1.93 (± 0.04)
425cm	-1.67 (± 0.04)
430cm	-1.66 (± 0.06)
435cm	-1.60 (± 0.12)
440cm	-1.63 (± 0.06)
449cm	-1.70 (± 0.06)
455cm	-1.64 (± 0.12)
460cm	-1.54 (± 0.04)
470cm	-1.42 (± 0.08)
480cm	-1.73 (± 0.08)
485cm	-1.72 (± 0.12)
490cm	-1.43 (± 0.12)
495cm	-1.77 (± 0.03)
500cm	-1.98 (± 0.08)
510cm	-1.53 (± 0.09)
520cm	-1.73 (± 0.09)

Supplementary Table 2: Radiocarbon measurements for sediment core KNR140-2-56GGC based on *Globigerinoides ruber*. All new measurements were carried out at NOSAMS on *G. ruber* (white). Calendar ages were calculated using Calib v.6.1.0, using Marine09 and a ΔR of 148 (±70).

Depth (cm)	Conventional radiocarbon age (kya BP)	Age error (1 sigma kya BP)	Min calendar age (1 sigma kya BP)	Max calendar age (1 sigma kya BP)
12.5[b]	1440	35	753	913
200	5340	40	5462	5631
400[a]	9800	55	10405	10596
415	12400	55	13584	13818
425[a]	14350	100	16873	17125
435	18600	95	21336	21732
442	14400	100	16809	17055
470	25500	110	29545	30156
495[b]	24700	120	28725	29230
510[a]	25100	240	28962	29648

a from [8]; b from J. F. McManus, unpublished

Supplementary Table 3: Boundary conditions and variables used in the box model. Note values for dissolution were estimated from [60].

PARAMETER	SYMBOL	MAGNITUDE/UNITS
Boundary conditions		
Area of ocean box (200 km^2)	A	$4X10^{10}$ m^2
Volume of intermediate box	V_{INT}	$4X10^{13}$ m^3
Volume of surface box	V_{SURF}	$4X10^{12}$ m^3
Concentration of upwelling water	C_{IN}	30 μM Si
Isotopic composition of E. rex	δ_{rex}	+1.1 ‰
Isotopic composition of radiolarians	δ_{rad}	+2.1 ‰
Isotopic composition of input	δ_{in}	+1.6 ‰
Fractionation by E. rex	ε_{rex}	-1.1 to -2.1 ‰
Fractonation by radiolarians	ε_{rad}	-0.9 to -2.1 ‰
Diapycnal turbulent diffusion coefficient	K_d	1×10^{-5} m^2 s^{-1}
Unknowns		
Flux of water in by upwelling	F_{IN}	
Flux of water in by diapycnal diffusion	F_{vd}	
Concentration of intermediate water	C_{INT}	
Concentration of surface water	C_{SURF}	
Fraction of Si utilised by E. rex	f_{rex}	
Fraction of Si utilised by radiolarians	f_{rad}	
Isotopic composition of intermediate water	δ_{int}	
Isotopic composition of surface water	δ_{surf}	
Export of Si by E. rex	ϕ_{rex}	
Export of Si by radiolarians	ϕ_{rad}	
Dissolution of radiolarians	P_{rad}	
Dissolution of E. rex	P_{rex}	